14-3-3 Protein Interacts with Nuclear Localization Sequence of Forkhead Transcription Factor FoxO4

Veronika Obsilova,[‡] Jaroslav Vecer,[§] Petr Herman,[§] Anna Pabianova,[‡,||] Miroslav Sulc,[⊥,#] Jan Teisinger,[‡] Evzen Boura,[‡,||] and Tomas Obsil*[,‡,||]

Department of Physical and Macromolecular Chemistry, Faculty of Science, Charles University, 12843 Prague, Czech Republic, Institute of Physiology, Academy of Sciences of the Czech Republic, 12843 Prague, Czech Republic, Institute of Physics, Faculty of Mathematics and Physics, Charles University, 12843 Prague, Czech Republic, Department of Biochemistry, Faculty of Science, Charles University, 12843 Prague, Czech Republic, and Institute of Microbiology, Academy of Sciences of the Czech Republic, 12843 Prague, Czech Republic

Received April 4, 2005; Revised Manuscript Received June 14, 2005

ABSTRACT: The 14-3-3 proteins are a family of regulatory signaling molecules that interact with other proteins in a phosphorylation-dependent manner. 14-3-3 proteins are thought to play a direct role in the regulation of subcellular localization of FoxO forkhead transcription factors. It has been suggested that the interaction with the 14-3-3 protein affects FoxO binding to the target DNA and interferes with the function of nuclear localization sequence (NLS). Masking or obscuring of NLS could inhibit interaction between FoxO factors and nuclear importing machinery and thus shift the equilibrium of FoxO localization toward the cytoplasm. According to our best knowledge, there is no experimental evidence showing a direct interaction between the 14-3-3 protein and NLS of FoxO. Therefore, the main goal of this work was to investigate whether the phosphorylation by protein kinase B, the 14-3-3 protein, and DNA binding affect the structure of FoxO4 NLS. We have used site-directed labeling of FoxO4 NLS with the extrinsic fluorophore 1,5-IAEDANS in conjunction with steady-state and time-resolved fluorescence spectroscopy to study conformational changes of FoxO4 NLS *in vitro*. Our data show that the 14-3-3 protein binding significantly changes the environment around AEDANS-labeled NLS and reduces its flexibility. On the other hand, the phosphorylation itself and the binding of double-stranded DNA have a small effect on the structure of this region. Our results also suggest that the DNA-binding domain of FoxO4 remains relatively mobile while bound to the 14-3-3 protein.

The forkhead box (Fox) class of transcription factors is a family of structurally related transcriptional activators that have been found in a variety of species ranging from yeast to humans (*1*−*4*). The common feature of all of the Fox class transcription factors is the presence of the forkhead box DNA-binding domain (DBD).[1] This domain comprises about 100 amino acid residues and is characterized by three α helices packed against each other and a small three-stranded β sheet from which two characteristic large wings protrude (*5*). The members of the "O" subfamily within the Fox protein family, which in mammals consist of FoxO1, FoxO3a, FoxO4, and FoxO6, participate in various cellular processes, including apoptosis, cell-cycle progression, and response to stress (*2*, *4*, *6*, *7*). The transcriptional activity of FoxO factors is controlled through the phosphatidylinositol 3-kinase−protein kinase B (PI3K−PKB) signaling pathway (*2*, *8*). PKB phosphorylates FoxO factors at three specific sites (Figure 1) and creates two binding sites for 14-3-3 proteins (*9*−*12*). PKB-mediated phosphorylation is followed by phosphorylation of additional sites by casein kinase 1 and rapid export of FoxO proteins from the nucleus.

The 14-3-3 proteins are a family of conserved regulatory molecules that interact with other proteins in a phosphorylation-dependent manner (*13*). 14-3-3 proteins function as molecular scaffolds, modulating the conformation of their binding partners (*14*−*18*). As a result of this structural modulation they can (i) affect the enzymatic properties of their partners, (ii) interfere with the protein−protein interactions of their targets, or (iii) regulate the subcellular localization of their binding partners presumably by masking or obscuring a nearby targeting sequence, such as a nuclear localization sequence (NLS) or a nuclear export sequence

* To whom correspondence should be addressed: Faculty of Science, Charles University, Prague, Czech Republic. Telephone: 420-221951303. Fax: 420-224919752. E-mail: obsil@natur.cuni.cz.

[‡] Institute of Physiology, Academy of Sciences of the Czech Republic.

[§] Institute of Physics, Faculty of Mathematics and Physics, Charles University.

[||] Department of Physical and Macromolecular Chemistry, Faculty of Science, Charles University.

[⊥] Department of Biochemistry, Faculty of Science, Charles University.

[#] Institute of Microbiology, Academy of Sciences of the Czech Republic.

[1] Abbreviations: 1,5-IAEDANS, 5-((((2-iodoacetyl)amino)ethyl)-amino)naphthalene-1-sulfonic acid; AEDANS, 5-(((acetylamino)ethyl)-amino)naphthalene-1-sulfonic acid; DBD, DNA-binding domain; MALDI−TOF, matrix-assisted laser desorption ionisation−time-of-flight; PSD, post source decay; MEM, maximum entropy method; SVD, singular value decomposition; $dpFoxO4_{11-213}$, doubly phosphorylated $FoxO4_{11-213}$; $pFoxO4_{82-207}$, phosphorylated $FoxO4_{82-207}$; PKB, protein kinase B; PI3K, phosphatidylinositol 3-kinase; NLS, nuclear localization sequence; WT, wild type.

10.1021/bi050618r CCC: $30.25
Published on Web 08/04/2005

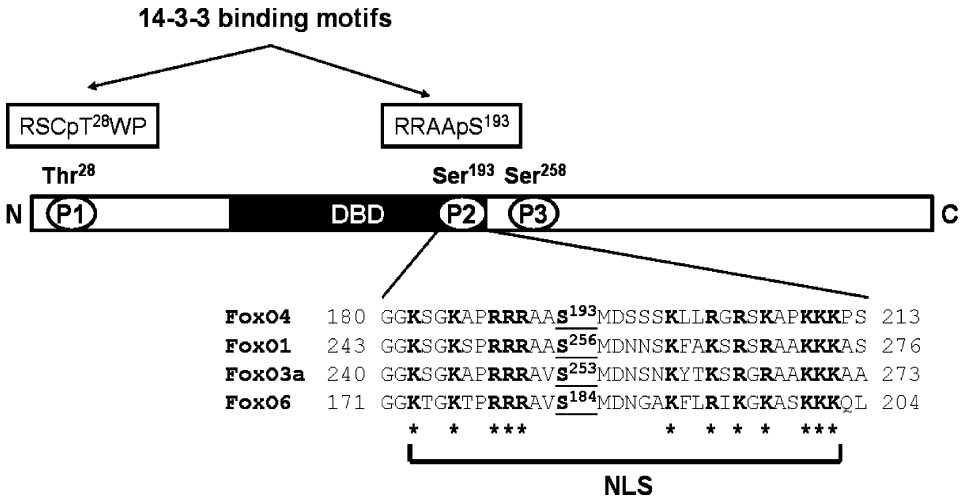

FIGURE 1: Diagram of the FoxO4 primary structure. The positions of PKB phosphorylation sites (P1, P2, and P3) and two 14-3-3 binding motifs are shown. The sequence alignment shows human FoxO4, FoxO1, FoxO3a, and mouse FoxO6 NLSs. Basic residues that form the NLS are bold and marked by stars.

(NES). The Cdc25 phosphatases (*19*), telomerase (*20*), or histone deacetylase (*21*) have been suggested to be subject to such regulation. All FoxO transcription factors contain a sequence that represents a nonclassical bipartite NLS. This NLS consists of 12 arginine and lysine residues surrounding the PKB phosphorylation motif located within the C-terminal region of DBD (Figure 1) (*22*, *23*). Given the presence of the PKB/14-3-3 binding motif in the vicinity of this NLS, it has been suggested that the 14-3-3 proteins participate in the regulation of subcellular localization of FoxO factors through the interference with the nuclear localization functions (*22*−*24*).

It is reasonable to speculate that such a mode of FoxO regulation likely requires a direct interaction between the 14-3-3 protein and NLS, which would mask the interaction between the NLS and nuclear import machinery. However, such an interaction between the 14-3-3 protein and FoxO NLS has not yet been shown. Our aim was to investigate whether the 14-3-3 protein interacts with and affects the structure of the C-terminal part of FoxO DBD where the NLS is located. We have used site-directed labeling of FoxO4 NLS with the extrinsic fluorophore 1,5-IAEDANS in conjunction with steady-state and time-resolved fluorescence spectroscopy to study the interaction between the 14-3-3 protein and the FoxO4 NLS *in vitro*. Fluorescence spectroscopy data show that the 14-3-3 protein binding significantly changes the environment around AEDANS-labeled NLS and reduces its flexibility. On the other hand, both the PKB phosphorylation by itself and the binding of double-stranded DNA have a small effect on the structure of this region of the FoxO4 molecule. Our results also suggest that the DBD of FoxO4 remains relatively mobile while bound to the 14-3-3 protein.

MATERIALS AND METHODS

Expression, Purification, and Phosphorylation of FoxO4. DNA-encoding human FoxO4 sequences 11−260 and 11−501 were inserted into pET-15b (Novagen) at the *Bam*HI site. $FoxO4_{11-213}$ was expressed, purified, and phosphorylated according to the protocol described previously (*11*). All $FoxO4_{11-213}$ and $FoxO4_{82-207}$ mutants were generated using the QuickChange kit (Stratagene). $FoxO4_{11-213}$ (WT or Cys mutant) was expressed as a GST-fusion protein by IPTG induction for 12 h at 20 °C and purified from *Escherichia coli* BL21(DE3) cells using GST-Sepharose 4B (Amersham Pharmacia Biotech) according to the standard protocol. The GST tag was cleaved by incubation (1 h at 30 °C) with TEV protease (Invitrogen). After the cleavage, $FoxO4_{11-213}$ was purified using cation-exchange chromatography on a HiTrap SP column (Amersham Pharmacia Biotech). The protein was eluted using 50−1000 mM NaCl gradient in 50 mM Na-citrate (pH 6.3), 1 mM DTT, and 1 mM EDTA. Fractions containing $FoxO4_{11-213}$ were dialyzed overnight against buffer containing 20 mM Tris (pH 7.5), 100 mM NaCl, 1 mM EDTA, and 1 mM DTT. $FoxO4_{82-207}$ has been expressed as a 6× His-tag-fusion protein by IPTG induction for 12 h at 30 °C and purified from *E. coli* BL21(DE3) cells using Chelating-Sepharose Fast Flow (Amersham Pharmacia Biotech) according to the standard protocol (*5*). The 6× His tag was cleaved by incubation (8 h at 4 °C) with thrombin (Sigma). After the cleavage, $FoxO4_{82-207}$ was purified using cation-exchange chromatography as $FoxO4_{11-213}$. Purified $FoxO4_{11-213}$ and $FoxO4_{82-207}$ were then phosphorylated by incubation (2 h at 30 °C) with 9 units of active PKBα (Upstate Biotechnology) per milligram of protein in the presence of 10 mM magnesium acetate and 0.2 mM ATP. After the phosphorylation, the $dpFoxO4_{11-213}$ and $pFoxO4_{82-207}$ were repurified using cation-exchange chromatography as mentioned above. Eluted proteins were finally dialyzed against buffer containing 20 mM Tris (pH 7.5), 100 mM NaCl, 1 mM EDTA, 2 mM DTT, and 10% (w/v) glycerol. The completeness of the phosphorylation reaction was checked using the MALDI−TOF mass spectrometry.

Mass Spectrometric Analysis. Samples were first separated by 12% SDS−PAGE, and excised protein bands were digested with trypsine (Promega) directly in gel (*25*). Resulting peptide mixtures were extracted by 30% acetonitrile and 0.3% acetic acid and subjected to MALDI−TOF mass spectrometer BIFLEX (Bruker-Franzen, Bremen, Germany) equipped with a nitrogen laser (337 nm) and gridless delayed extraction ion source. Ion acceleration voltage was 19 kV, and the reflectron voltage was set to 20 kV. Spectra were calibrated externally using the monoisotopic $[M + H]^+$ ion of peptide standards angiotensin I (Sigma). A saturated

solution of α-cyano-4-hydroxy-cinnamic acid in 50% MeCN/0.3% acetic acid was used as a MALDI matrix. A total of 1 μL of matrix solution was mixed with 1 μL of the sample on the target, and the droplet was allowed to dry at ambient temperature.

Labeling of FoxO4$_{11-213}$ by 1,5-IAEDANS. Human FoxO4 (fragment 11−213) possesses 1 cysteine residue (Cys^{27}). To prepare FoxO4$_{11-213}$ specifically labeled with fluorescence probe at the end of its nuclear localization sequence, we mutated Cys^{27} to Ala and inserted a new Cys residue to position 213 (mutation Ser^{213}Cys). Covalent modification of FoxO4$_{11-213}$ containing a single cysteine residue at position 213 with thiol-reactive probe 1,5-IAEDANS was carried out as described elsewhere (*26*). Briefly, the protein (50−70 μM) in 50 mM Tris (pH 7.5), 100 mM NaCl, and 1 mM EDTA and label were mixed at a molar ratio of 1:40 and incubated at 30 °C for 2 h and then at 4 °C overnight in the dark. The free unreacted label was removed by gel filtration in buffer containing 50 mM Tris (pH 7.5), 100 mM NaCl, and 1 mM EDTA. The incorporation stoichiometry was determined by the absorbance at 336 nm using an extinction coefficient of 5700 M^{-1} cm^{-1} (Molecular Probes, Eugene, OR).

Tryptophan Mutagenesis of FoxO4$_{82-207}$. To use intrinsic fluorescence to monitor the flexibility of FoxO4 DBD, we have prepared a mutant of FoxO4$_{82-207}$ containing only two Trp residues at positions 173 and 174 located within the DBD (*5*). Other tryptophan residues were mutated to phenylalanine. After each mutation (Trp^{97}Phe, Trp^{126}Phe, and Trp^{146}Phe), the DNA-binding ability of mutated FoxO4$_{82-207}$ has been tested using the electrophoretic mobility shift assay.

Expression and Purification of the 14-3-3 Protein. Human 14-3-3 protein (ζ isoform) was expressed and purified as described previously (*11, 17*).

Electrophoretic Mobility Shift Assay. Samples containing 250 pmol of FoxO4$_{11-213}$ or phosphorylated dpFoxO4$_{11-213}$ protein and 500 pmol of 14-3-3 protein were incubated with 300 pmol of double-stranded DNA (sequence 5′-GCAAAACAAAC-3′) for 30 min at 4 °C in a buffer containing 20 mM Tris (pH 7.5), 100 mM NaCl, 1 mM EDTA, and 2 mM DTT. Samples were resolved on native 12% TBE−PAGE at 200 V. Gels were silver-stained for DNA visualization (*27*). Gels were analyzed using the public domain software package ImageJ (NIH).

Steady-State Fluorescence Measurements. Steady-state fluorescence measurements were performed on a Perkin−Elmer LS50B fluorescence spectrometer at 22 °C with 4 μM FoxO4$_{11-213}$ or dpFoxO4$_{11-213}$ labeled with 1,5-IAEDANS at Cys^{213} in 50 mM Tris (pH 7.5), 100 mM NaCl, and 1 mM EDTA buffer. Increasing amounts of 14-3-3 protein were titrated into the cuvette. At each 14-3-3 concentration, the steady-state fluorescence anisotropy of AEDANS was measured (excitation at 336 nm and emission at 490 nm). Anisotropy was calculated from the fluorescence intensities according to the relationship $r = (I_{||} - I_{\perp})/(I_{||} + 2I_{\perp})$. The fraction of FoxO4 bound (F_B) was calculated from the formula

$$F_B = (r_{obs} - r_{min})/[(r_{max} - r_{obs})Q + (r_{obs} - r_{min})], \quad (1)$$

where Q represents the quantum yield ratio of the bound to the free form and was estimated by the ratio of the intensities of the bound to the free fluorophore. Parameter r_{max} is the anisotropy at saturation; r_{obs} is the observed anisotropy for any 14-3-3 protein concentration; and r_{min} is the minimum observed anisotropy. F_B was plotted against the 14-3-3 protein concentration and fitted using eq 2 to determine the K_D for the dpFoxO4$_{11-213}$/14-3-3 protein complex formation

$$F_B = \{K_D + [P1] + [P2] - \sqrt{(K_D + [P1] + [P2])^2 - 4[P1][P2]}\}/2[P1] \quad (2)$$

where K_D is the equilibrium dissociation constant, $P1$ is the dpFoxO4−AEDANS concentration, and $P2$ is the 14-3-3 protein concentration. Nonlinear data fitting was performed using the Origin 6.0 package (Microcal Software Inc.).

Time-Resolved Fluorescence Measurements. Fluorescence intensity decays were measured on an apparatus described previously (*28*). Fluorescence decays have been acquired under the "magic angle" conditions when the measured intensity decay $I(t)$ is independent of a rotational diffusion of the chromophore and provides unbiased information about lifetimes. The apparatus response function was measured with a diluted Ludox solution. Samples were placed in a thermostatic holder, and all experiments were performed at 15 °C in buffer containing 50 mM Tris-HCl (pH 7.5), 100 mM NaCl, and 1 mM EDTA. FoxO4$_{11-213}$ and dpFoxO4$_{11-213}$ concentrations were 15 μM; the 14-3-3 protein concentration was 30 μM; and the double-stranded DNA (sequence 5′-GCAAAACAAAC-3′) concentration was 17 μM. Dansyl fluorescence was excited and collected at 315 and 480 nm, respectively. Tryptophan emission was excited at 298 nm and collected at 360 nm. Fluorescence decays were processed as described previously (*28*) using the singular-value-decomposition maximum entropy method (SVD-MEM) (*28*). For a multiexponential fluorescence decay $I(t)$, the program returns set of amplitudes α_i, which represent a distribution of the corresponding lifetimes τ_i

$$I(t) = \sum_i \alpha_i e^{-t/\tau_i} \quad (3)$$

The mean lifetimes were calculated from the formula

$$\tau_{mean} = \sum_i \alpha_i \tau_i^2 / \sum_i \alpha_i \tau_i \quad (4)$$

The fluorescence anisotropy decays $r(t)$ were obtained from the parallel $I_{||}(t)$ and perpendicular $I_{\perp}(t)$ decay components. Data were analyzed by a method similar to the one published by Brochon (*30*) using the program developed at the Institute of Physics, Charles University, Prague, Czech Republic. We have used a model independent SVD-MEM approach that does not set prior limits on the shape of the distribution. The anisotropies were analyzed for a series of exponentials

$$r(t) = \sum_i \beta_i e^{-t/\phi_i} \quad (5)$$

where the amplitudes β_i represent a distribution of the correlation times ϕ_i. The β_i are related to the initial anisotropy r_0 by the formula

$$\sum_i \beta_i = r_0 \quad (6)$$

We used 150 correlation times ϕ_l equidistantly spaced in the logarithmic scale and ranging from 100 ps to 500 ns. For complex distributions, the mean correlation time associated with the *m*th peak of the distribution was calculated from the formula

$$\bar{\phi}_m = \sum_k \beta_k \phi_k / \sum_i \beta_k \quad (7)$$

where the index *k* runs over the nonzero amplitudes of the *m*th peak of the distribution only. The area of the peak represents the associated mean amplitude $\bar{\beta}_m$.

RESULTS

Preparation and Characterization of Labeled FoxO4$_{11-213}$ Mutants. To study the effect of the 14-3-3 protein binding on the structure of FoxO4 NLS, a construct containing human FoxO4 sequence 11−213 (FoxO4$_{11-213}$) has been used (*11*) to prepare a mutant suitable for site-specific labeling of NLS. This construct covers the N-terminal half of the FoxO4 protein and contains the forkhead DBD flanked by two PKB phosphorylation/14-3-3 protein binding sites and predicted bipartite NLS (Figure 1). We have also attempted to express two longer versions of human FoxO4 transcription factor (sequences 11−260 and 11−501) as histidine-tagged fusion proteins. However, expression test revealed that these constructs (FoxO4$_{11-260}$ and FoxO4$_{11-501}$) could not be expressed in *E. coli* BL21(DE3) cells because of the very low expression yield or the high proteolytic degradation of the recombinant protein during the expression under all conditions tested.

The amino acid sequence of FoxO4$_{11-213}$ contains one cysteine residue at position 27. To specifically label the NLS of FoxO4$_{11-213}$ with a fluorescence probe, we have mutated Cys^{27} to Ala and introduced a new Cys residue at position 213. Cystein 213 was then labeled with the extrinsic fluorophore 1,5-IAEDANS, and the stoichiometry of AEDANS incorporation per mole of the FoxO4$_{11-213}$ was found to be 95−98%. AEDANS-labeled FoxO4$_{11-213}$ was phosphorylated using PKB, which is known to stechiometrically phosphorylate FoxO4$_{11-213}$ *in vitro* at two sites Thr^{28} and Ser^{193} (*11*). The completeness of phosphorylation was determined using the MALDI−TOF mass spectrometry. Negative and positive ion mass spectra were measured in the reflection mode to check the amino acid sequences of phosphorylated FoxO4$_{11-213}$ tryptic peptides. The comparison of negative MALDI−TOF mass spectra of trypsinised unphosphorylated and phosphorylated FoxO4$_{11-213}$ clearly demonstrates the presence of phosphorylated peptides. The detected peak in negative ion mass spectra of phosphorylated FoxO4$_{11-213}$ mutant having the mass of 961.4 (*m*/*z*) corresponds to phosphorylated peptide AASMDSSSK (C-terminal PKB phosphorylation site). On the other hand, unphosphorylated protein provided a peak of intact peptide with *m*/*z* 881.4 there. Moreover, the identified peak of 3161.5 (*m*/*z*) fits to the peptide sequence SATWPLPRPEIANQPSEPPEVEPDLGEK (*m*/*z* 3081.5) with one phosphate group (N-terminal PKB phosphorylation site with a Cys^{27} to Ala mutation). The identity and structure of phosphorylated tryptic peptides were further corroborated by analysis of their PSD spectra to authenticate Thr^{28} and Ser^{193} as phosphorylated amino acid residues (data not shown).

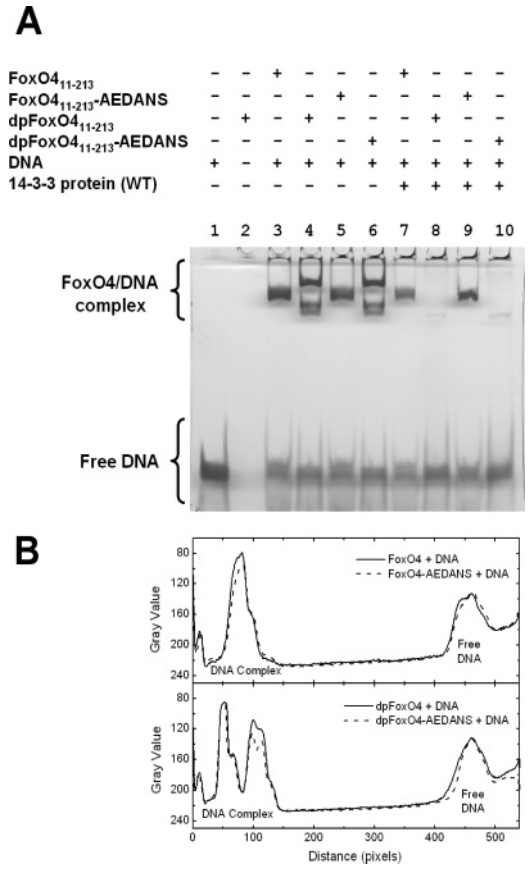

FIGURE 2: (A) Labeling with 1,5-IAEDANS does not affect DNA-binding properties of FoxO4$_{11-213}$ nor its interaction with the 14-3-3 protein. Native 12% TBE−PAGE electrophoresis, silver staining for DNA. Labeling with 1,5-IAEDANS does not affect the binding of FoxO4$_{11-213}$ to target DNA (compare lanes 3 and 5 and 4 and 6). The 14-3-3 protein inhibits DNA binding of phosphorylated dpFoxO4$_{11-213}$ but not unphosphorylated FoxO4$_{11-213}$ (compare lanes 4 and 8 and 6 and 10). FoxO4$_{11-213}$, DNA, and the 14-3-3 protein were mixed in a 1:1.2:2 molar ratio. (B) Lane profile plots of TBE gel patterns for lanes 3−5 and 4−6. Integration of peaks corresponding to the FoxO4/DNA complex revealed that modification of Cys^{213} by 1,5-IAEDANS has no significant effect on DNA binding of both FoxO4$_{11-213}$ and dpFoxO4$_{11-213}$.

Modification of Cys^{213} by 1,5-IAEDANS Does Not Affect DNA-Binding Properties of FoxO4 nor Its Interaction with the 14-3-3 Protein. Electrophoretic mobility shift assay was used to check the DNA-binding properties of AEDANS-labeled FoxO4$_{11-213}$ and dpFoxO4$_{11-213}$ (Figure 2A). Lane profile plots of DNA-binding patterns of unlabeled and labeled FoxO4 (lanes 3 and 5) and dpFoxO4 proteins (lanes 4 and 6) show that modification of Cys^{213} by 1,5-IAEDANS has no significant effect on their DNA-binding properties (Figure 2B). Recently, it has been demonstrated that binding of the 14-3-3 protein significantly inhibits dpFoxO4$_{11-213}$ binding to its target DNA (*11*). Similar 14-3-3-dependent inhibition of DNA binding was observed for both unlabeled and AEDANS-labeled versions of phosphorylated dpFoxO4$_{11-213}$ (lanes 8 and 10), while unphosphorylated FoxO4$_{11-213}$ retains its ability to bind DNA in the presence of the 14-3-3 protein (lanes 7 and 9). These data indicate that the insertion of Cys^{213} and its modification with 1,5-IAEDANS does not interfere with the binding of dpFoxO4$_{11-213}$ to the 14-3-3 protein. The ability of AEDANS-labeled dpFoxO4$_{11-213}$ to bind to 14-3-3 protein was further confirmed using the steady-state measurements of Cys^{213}-

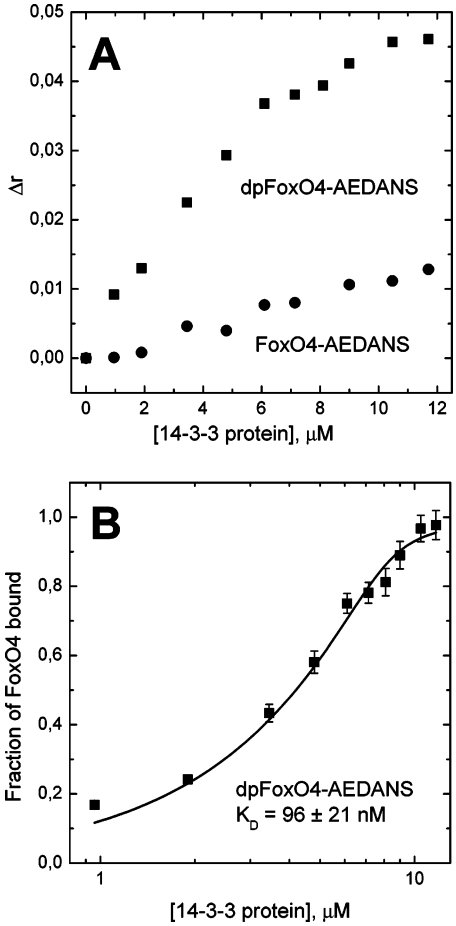

FIGURE 3: 14-3-3 protein binds to the AEDANS-labeled phosphorylated dpFoxO4 with high affinity. (A) Comparison of the change in steady-state anisotropy, *r*, upon addition of the 14-3-3 protein to the AEDANS-labeled phosphorylated dpFoxO4 (■) and unphosphorylated FoxO4 (●). (B) Data for the curve with AEDANS-labeled phosphorylated dpFoxO4 could be fitted to yield a dissociation constant of 96 ± 21 nM.

AEDANS emission anisotropies (Figure 3). Binding of the 14-3-3 protein to the phosphorylated dpFoxO4$_{11-213}$ significantly increased the steady-state anisotropy of Cys^{213}-AEDANS as a result of the dpFoxO4$_{11-213}$/14-3-3 complex formation (Figure 3A). If we consider the dpFoxO4$_{11-213}$/14-3-3 complex with a 1:2 molar stoichiometry (*11*), the data for this curve could be fitted to yield a dissociation constant of 96 ± 21 nM (Figure 3B). On the other hand, the titration of the 14-3-3 protein to the unphosphorylated FoxO4$_{11-213}$, which is known to interact with the 14-3-3 protein with very low affinity (*11*), had a small effect on the steady-state fluorescence anisotropy of Cys^{213}-AEDANS.

14-3-3 Protein Binding Affects the Polarity around the AEDANS-Labeled NLS of dpFoxO4. It has been suggested that the 14-3-3 protein binding might interfere with the function of FoxO4 NLS (*9*, *12*, *24*). Such molecular interference could be based on a conformational change of NLS, which masks or obscures the interaction between the NLS and nuclear import machinery. To monitor local conformational changes of FoxO4 NLS, the fluorescent label, AEDANS, was attached to Cys^{213}. Figure 4 illustrates representative fluorescence emission spectra of Cys^{213}-AEDANS from FoxO4$_{11-213}$ and their changes upon the binding of DNA and the 14-3-3 protein. The binding of DNA slightly decreased the fluorescence intensity of Cys^{213}-

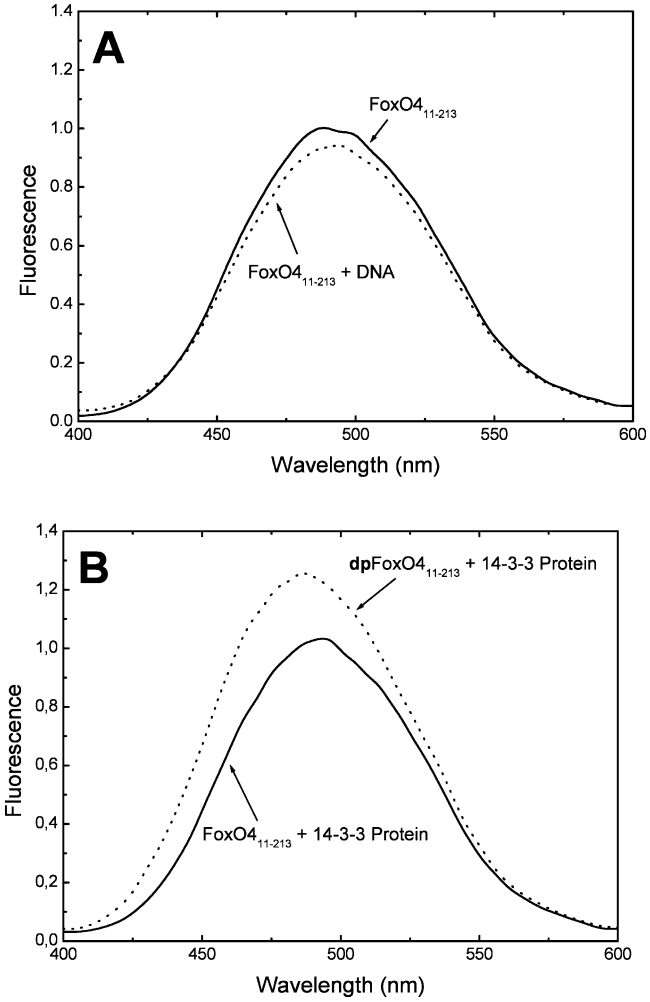

FIGURE 4: Steady-state fluorescence emission spectra of FoxO4 NLS-Cys^{213}-AEDANS. (A) Effect of DNA binding on fluorescence emission of AEDANS-labeled NLS of unphosphorylated FoxO4$_{11-213}$. (—) Spectrum in the absence of DNA. (•••) Spectrum in the presence of DNA. (B) Effect of the 14-3-3 protein binding on fluorescence emission of AEDANS-labeled NLS. (—) Spectrum of unphosphorylated FoxO4$_{11-213}$ in the presence of the 14-3-3 protein. (•••) Spectrum of doubly phosphorylated dpFoxO4$_{11-213}$ in the presence of the 14-3-3 protein. Only phosphorylated dpFoxO4$_{11-213}$ binds to the 14-3-3 protein. In both A and B, the spectra were normalized by the peak intensity of the unphosphorylated FoxO4$_{11-213}$.

AEDANS both for unphosphorylated FoxO4$_{11-213}$ (Figure 4A) and doubly phosphorylated dpFoxO4$_{11-213}$ (data not shown). On the other hand, the 14-3-3 protein binding to the dpFoxO4$_{11-213}$ caused about 25% enhancement of Cys^{213}-AEDANS fluorescence accompanied with a blue shift of the emission maximum from 494 to 486 nm (Figure 4B). Both the increase in the fluorescence intensity and the corresponding blue shift of fluorescence maxima indicate a significant decrease in the polarity around the AEDANS group attached to Cys^{213} of dpFoxO4$_{11-213}$ upon the binding of the 14-3-3 protein. Phosphorylation itself has no significant effect on steady-state fluorescence emission of Cys^{213}-AEDANS (data not shown).

To obtain more detailed information about structural changes of AEDANS-labeled NLS, we performed time-resolved fluorescence intensity and anisotropy decay measurements of Cys^{213}-AEDANS. Figure 5 shows the effect of DNA and 14-3-3 protein binding on the fluorescence lifetime distribution of Cys^{213}-AEDANS. AEDANS is an environ-

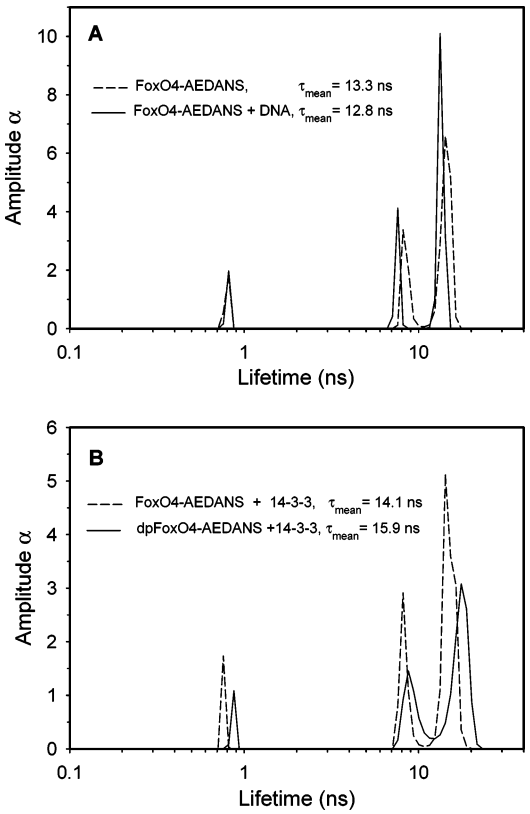

FIGURE 5: Effect of DNA and 14-3-3 protein binding on the fluorescence lifetime distribution of NLS-Cys^{213}-AEDANS. (A) Comparison of fluorescence lifetime distributions of AEDANS-labeled unphosphorylated FoxO4$_{11-213}$ in the absence (—) and presence (- - -) of DNA. (B) Comparison of fluorescence lifetime distributions of AEDANS-labeled phosphorylated dpFoxO4$_{11-213}$ (—) and AEDANS-labeled unphosphorylated FoxO4$_{11-213}$ (- - -) in the presence of the 14-3-3 protein.

mentally sensitive fluorophore that changes its lifetime according to local interactions of the fluorophore. We have found that the intensity decays of Cys^{213}-AEDANS for all FoxO4$_{11-213}$ samples can be adequately described by a trimodal lifetime distribution. The binding of DNA somewhat reduces the mean excited-state lifetime, τ_{mean}, of Cys^{213}-AEDANS from 13.3 to 12.8 ns (Figure 5A), with the effect being independent of the FoxO4$_{11-213}$ phosporylation (data not shown). An opposite effect was found in the presence of the 14-3-3 protein when in the case of the unphosphorylated FoxO4$_{11-213}$ τ_{mean} increases from 13.3 to 14.1 ns. The lifetime increase is highly enhanced after phosporylation when τ_{mean} increases up to 15.9 ns after the binding of the dpFoxO4$_{11-213}$ to the 14-3-3 protein (Figure 5B). The overall pattern of Cys^{213}-AEDANS lifetime distribution is independent of the phosphorylation and the ligand binding. The changes of τ_{mean} upon the 14-3-3 protein or DNA binding are in agreement with the results of the steady-state fluorescence measurements. Data indicate changes of the microenvironment around the AEDANS-labeled NLS of dpFoxO4$_{11-213}$, with the microenvironment being significantly less and slightly more polar in the presence of the 14-3-3 protein and DNA, respectively.

14-3-3 Protein Binding Reduces the Flexibility of AEDANS-Labeled NLS of dpFoxO4. To obtain detailed information on the mobility of FoxO4 NLS, the time-resolved fluorescence anisotropy decay measurements of Cys^{213}-AEDANS have been performed both in the presence and absence of

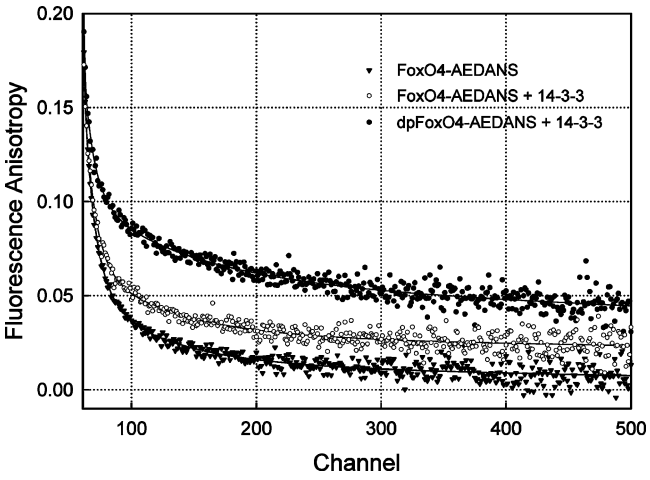

FIGURE 6: 14-3-3 protein binding reduces the flexibility of AEDANS-labeled NLS of dpFoxO4. Fluorescence anisotropy decays of Cys^{213}-AEDANS in the absence (▼) or presence (○ and ●) of the 14-3-3 protein. (○) Decay of the unphosphorylated FoxO4$_{11-213}$. (●) Decay of the phosphorylated dpFoxO4$_{11-213}$. (—) Least-squares fit of the data.

the 14-3-3 protein and DNA. The raw anisotropy data presented in Figure 6 show the effect of the 14-3-3 protein binding on the fluorescence anisotropy decay of Cys^{213}-AEDANS. It is seen that all anisotropy decays are heterogeneous with significant fractions of fast depolarization components. Visual inspection of Figure 6 clearly reveals that, in the presence of the 14-3-3 protein, the anisotropy of AEDANS-labeled dpFoxO4$_{11-213}$ decays to apparently higher limiting value at long times compared to the unphosphorylated FoxO4$_{11-213}$. Such data indicate a lower extent of the fast depolarizing movements, which is a consequence of more restricted segmental motion of Cys^{213}-AEDANS upon the binding of the 14-3-3 protein to the phosphorylated dpFoxO4$_{11-213}$. The highest depolarization was found for the FoxO4$_{11-213}$ in the absence of the 14-3-3 protein, with the effect being essentially independent of the protein phosphorylation. The quantitative MEM analysis revealed that the AEDANS moiety attached at Cys^{213} is highly mobile and exhibits rather heterogeneous anisotropy decays (Figure 7 and Table 1). All measured anisotropy decays of Cys^{213}-AEDANS were adequately described by a distribution containing four peaks. The two "fast" decay components with the mean correlation times of ~0.2 and 0.7−0.9 ns reflect fast motion of the fluorophore itself and depolarization caused by a segmental motion of the protein, respectively (*31*, *32*). The "slow" decay components exhibiting mean correlation times in the range of 4.5−6.3 and 30−150 ns reflect rotational movement of the whole protein. Assuming that the whole molecule rotates as a rigid body, the presence of multiple long correlation times could indicate a distinct dimensional asymmetry of the FoxO4$_{11-213}$ molecule and its complexes with the 14-3-3 protein and DNA (*32*, *33*). Alternatively, the two long correlation times could result from a superposition of independent movements of rigid subdomains of the protein or the complex. PKB phosphorylation by itself has a negligible effect on the Cys^{213}-AEDANS fluorescence anisotropy decays. The 14-3-3 protein binding to the phosphorylated dpFoxO4$_{11-213}$ significantly reduces fast movements of AEDANS-labeled NLS as documented by a decrease in the sum of $\beta_1 + \beta_2$ amplitudes (Table 1 and Figure 8, compare dpFoxO4 and dpFoxO4 and

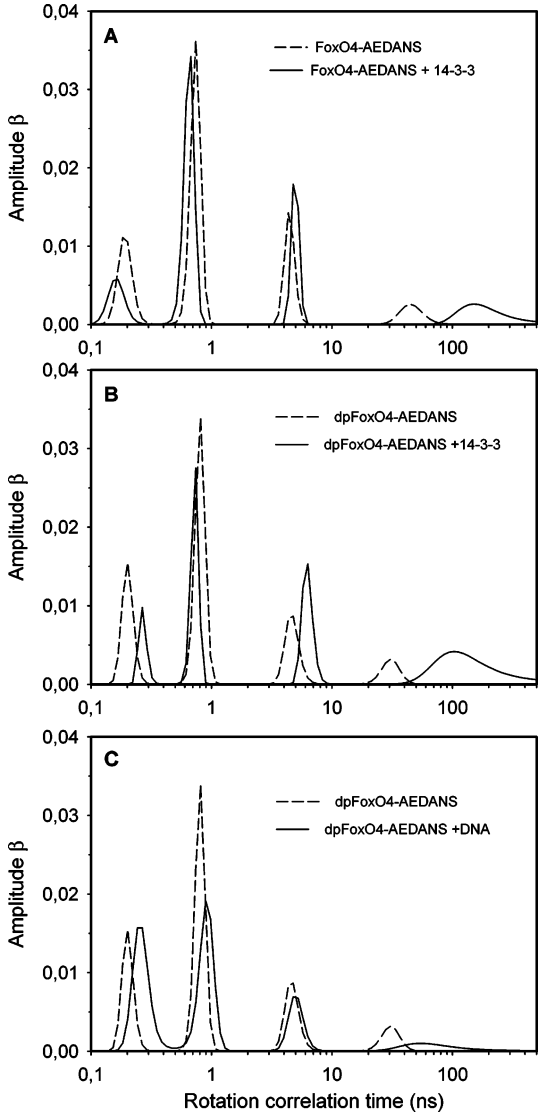

FIGURE 7: Distributions of rotational correlation times of Cys^{213}-AEDANS. (A) Distribution of rotational correlation times of the unphosphorylated $FoxO4_{11-213}$ in the absence (- - -) or presence (—) of the 14-3-3 protein. (B) Distribution of the phosphorylated $dpFoxO4_{11-213}$ in the absence (- - -) or presence (—) of the 14-3-3 protein. (C) Distribution of the phosphorylated $dpFoxO4_{11-213}$ in the absence (- - -) or presence (—) of DNA.

14-3-3). An advantage of the simultaneous evaluation of the cumulative amplitude β_1 and β_2 is a lower uncertainty of the sum compared to the uncertainty of the individual components caused by a partial correlation of the two peaks. The complex formation between dpFoxO4 and the 14-3-3 protein significantly increases both long correlation times $\bar{\phi}_3$ and $\bar{\phi}_4$ from 4.7 to 6.3 and 30 to 100 ns, respectively. These changes correspond with an increased molecular

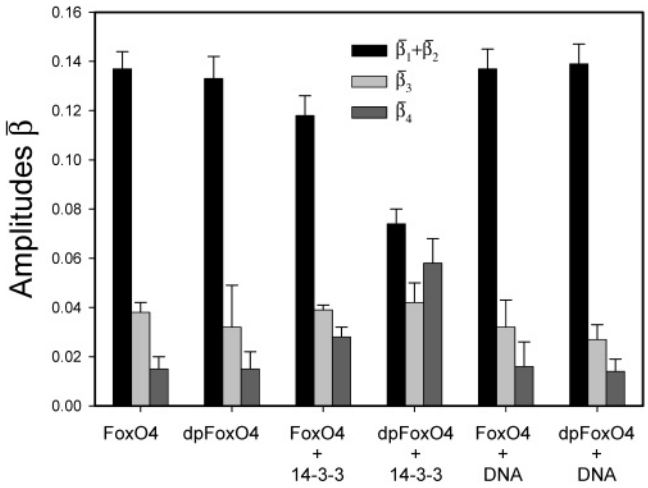

FIGURE 8: Proportional representation of the mean amplitudes $\bar{\beta}_i$ associated with the *i*th component $\bar{\phi}_i$ of the rotational correlation time distribution. Relation between the initial anisotropy and the amplitudes $\bar{\beta}_i$ is $r_0 = \sum_1^4 \bar{\beta}_i$. The sum $\bar{\beta}_1 + \bar{\beta}_2$ represents the cumulative amplitude of the fast Cys^{213}-AEDANS motions.

weight of dpFoxO4 upon the 14-3-3 protein binding (*34*).

Forkhead Domain of $dpFoxO4_{11-213}$ Remains Relatively Mobile upon the 14-3-3 Protein Binding. It is worth noting that a rotation of the molecule with a shape of a prolate ellipsoid of revolution exhibits three distinct long correlation times. The shortest of them is essentially independent of the molecular shape and roughly equals the correlation time of the equivalent isotropic rotor. The middle correlation time is relatively close to the shortest one and increases only slightly with increasing molecular asymmetry (*35*). It is extremely difficult to resolve those two correlation times in complex anisotropy decays with multiple depolarization processes, and we expect that these two correlation times are represented by $\bar{\phi}_3$ in our decays. The longest correlation time increases dramatically as the axial ratio of the molecule increases. This correlation time corresponds to $\bar{\phi}_4$, and it is determined by the rotation that displaces the long axis of the molecule. Because the $\bar{\phi}_3$ behaves as the correlation time of the equivalent spherical protein, the measured values of 4.7 and 6.3 ns would correspond to a protein with a molecular mass of approximately 10−13 kDa, respectively (*34*, *36*). This is about half of what we expect for our 22.5-kDa $FoxO4_{11-213}$. We conclude that this value is inconsistent with the model assuming the $FoxO4_{11-213}$ to be a rigid asymmetric rotor, and the correlation component with the $\bar{\phi}_3$ close to 5 ns reflects movement of a certain rigid domain within the $FoxO4_{11-213}$ construct. We assume that this could be compact and about 11 kDa large FoxO4 DBD (*5*). The same conclusion can be made from the fluorescence anisotropy of tryptophan residues measured on a different FoxO4

Table 1: Rotational Correlation Times of Cys^{213}-AEDANS of the Unphosphorylated $FoxO4_{11-213}$ and Phosphorylated $dpFoxO4_{11-213}$ in the Absence or Presence of the 14-3-3 Protein and DNA

sample	$\bar{\beta}_1$[a]	$\bar{\phi}_1$ (ns)	$\bar{\beta}_2$	$\bar{\phi}_2$ (ns)	$\bar{\beta}_3$	$\bar{\phi}_3$ (ns)	$\bar{\beta}_4$	$\bar{\phi}_4$ (ns)
FoxO4	0.042 ± 0.013	0.20	0.095 ± 0.012	0.70	0.038 ± 0.004	4.5	0.015 ± 0.005	45
dpFoxO4	0.045 ± 0.014	0.20	0.088 ± 0.012	0.80	0.032 ± 0.017	4.7	0.015 ± 0.007	30
FoxO4/14-3-3	0.025 ± 0.015	0.20	0.093 ± 0.013	0.70	0.039 ± 0.002	5.0	0.028 ± 0.004	150
dpFoxO4/14-3-3	0.020 ± 0.022	0.25	0.054 ± 0.021	0.70	0.042 ± 0.008	6.3	0.058 ± 0.010	100
FoxO4/DNA	0.056 ± 0.023	0.25	0.081 ± 0.022	0.80	0.033 ± 0.011	5.1	0.016 ± 0.010	60
dpFoxO4/DNA	0.069 ± 0.020	0.25	0.070 ± 0.019	0.90	0.027 ± 0.006	5.1	0.014 ± 0.005	55

[a] Relation between the initial anisotropy and the amplitudes $\bar{\beta}_i$ is $r_0 = \sum_1^4 \bar{\beta}_i$.

Table 2: Rotational Correlation Times of $Trp^{173,174}$ of the Unphosphorylated $FoxO4_{82-207}$ and Phosphorylated $pFoxO4_{82-207}$ in the Absence or Presence of the 14-3-3 Protein

sample	$\bar{\beta}_1$[a]	$\bar{\phi}_1$ (ns)	$\bar{\beta}_2$	$\bar{\phi}_2$ (ns)	$\bar{\beta}_3$	$\bar{\phi}_3$ (ns)	$\bar{\beta}_4$	$\bar{\phi}_4$ (ns)
FoxO4	0.001 ± 0.005	<0.2	0.070 ± 0.004	1.0	0.132 ± 0.012	4.1	0.037 ± 0.002	17.0
pFoxO4	0.008 ± 0.007	<0.2	0.059 ± 0.004	1.0	0.125 ± 0.002	3.6	0.051 ± 0.001	15.0
FoxO4/14-3-3	0.019 ± 0.005	<0.2	0.065 ± 0.011	1.3	0.109 ± 0.010	5.0	0.045 ± 0.011	15−200
pFoxO4/14-3-3	0.031 ± 0.005	<0.2	0.050 ± 0.006	1.2	0.105 ± 0.016	4.9	0.054 ± 0.007	15−200

[a] Relation between the initial anisotropy and the amplitudes $\bar{\beta}_i$ is $r_0 = \sum_1^4 \bar{\beta}_i$.

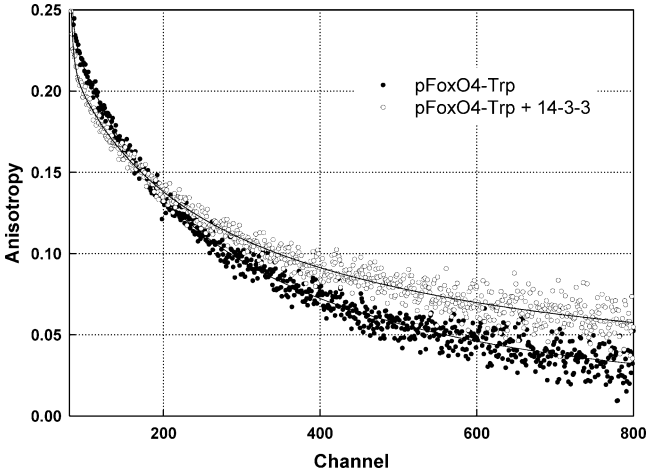

FIGURE 9: Tryptophan fluorescence anisotropy decays of $pFoxO4_{82-207}$ containing only $Trp^{173,174}$ in the absence (●) and presence (○) of 14-3-3. The scale is 14.6 ps/channel.

construct ($FoxO4_{82-207}$) containing only DBD with two tryptophan residues Trp^{173} and Trp^{174} and one 14-3-3 binding motif around PKB phosphorylation site Ser^{193} (Table 2 and Figure 9). In this suggested model, the longest correlation time $\bar{\phi}_4$ reflects the slowest depolarization process caused by a rotation of the molecule as a whole and clearly indicates formation of the $dpFoxO4_{11-213}$/14-3-3 protein (Table 1) or $pFoxO4_{82-207}$/14-3-3 protein complexes (Table 2). Data in Table 1 show that even though the unphosphorylated FoxO4 somehow interacts with the 14-3-3 protein, the fraction of the complex is low compared the phosphorylated counterpart (Figure 6). In conclusion, our data indicate that upon the 14-3-3 protein binding the forkhead domain of $dpFoxO4_{11-213}$ remains relatively mobile. If the dpFoxO4 binding to the 14-3-3 protein creates a rigid complex, then the $\bar{\phi}_3$ component should disappear or increase its value significantly more than it was found in our data.

DISCUSSION

Several groups have shown that 14-3-3 proteins play a direct role in the regulation of subcellular localization of FoxO proteins (*9*, *10*, *12*, *24*, *37*). In the absence of PKB activity, the FoxO proteins are predominantly localized within the nucleus and are presumed to be active. PKB phosphorylates FoxO proteins at three conserved residues and creates two binding sites for the 14-3-3 protein (*9*−*12*, *24*). Binding of the 14-3-3 protein is followed by rapid relocalization of the resulting complex into the cytoplasm. Once in the cytoplasm, FoxO factors remain phosphorylated and bound to the 14-3-3 proteins. It has been suggested that the interaction with the 14-3-3 protein can affect both FoxO binding to the target DNA (*11*, *37*) and nuclear localization functions of the NLS of FoxO (*12*, *18*, *24*). Masking or obscuring of NLS could inhibit interaction between FoxO factors and nuclear importing machinery and thus shifts the equilibrium of FoxO localization toward the cytoplasm. However, there is no experimental evidence showing direct interaction between the 14-3-3 protein and FoxO NLS. In this work, we have used fluorescence spectroscopy techniques to study whether the phosphorylation by PKB, the 14-3-3 protein binding, and the binding of double-stranded DNA affect the conformation of FoxO4 NLS.

Effect of the Phosphorylation by PKB. Our measurements revealed that PKB phosphorylation of Ser^{193} does not affect fluorescence properties of Cys^{213}-AEDANS (Figure 8 and Table 1). This indicates no significant alterations in the structure of the FoxO4 NLS region.

Effect of the 14-3-3 Protein Binding. The NLS of FoxO4 consists of 12 lysine and arginine residues that surround the P2 PKB phosphorylation site at the C terminus of DBD (Figure 1) (*22*, *23*). To study conformational changes in this region of FoxO4, we have inserted a Cys residue at position 213 and modified it with an extrinsic fluorophore 1,5-IAEDANS. Our measurements show that the 14-3-3 protein binding to phosphorylated $dpFoxO4_{11-213}$ (i) significantly decreases the polarity of the microenvironment around the AEDANS-labeled NLS and (ii) significantly reduces fast segmental movements of AEDANS-labeled NLS. These results strongly suggest that the 14-3-3 protein interacts with the NLS of $dpFoxO4_{11-213}$ and significantly affects its conformation. AEDANS-labeled Cys^{213} is located 20 amino acid residues downstream from the P2 PKB/14-3-3 motif "RRAApS^{193}MD". Crystal structures of 14-3-3 protein complexes with phosphopeptides (*38*, *39*) and serotonin *N*-acetyltransferase (*17*) showed that the 14-3-3 ligand-binding groove can accommodate a polypeptide chain about 9 amino acid residues long with the pS or pT in the middle. Therefore, the first part of FoxO4 bipartite NLS, three arginine residues located upstream to the PKB P2 site, would likely be directly buried within the ligand-binding groove upon the 14-3-3 protein binding. However, the second part of FoxO4 NLS consisting of 7 basic residues located between Lys^{199} and Lys^{211} is far enough from the P2 PKB/14-3-3 motif to be buried within the 14-3-3 ligand-binding groove. Significant reduction of fast segmental movements of AEDANS-labeled Cys^{213} (Figure 8 and Table 1) together with changes in the polarity of the microenvironment around this group (Figures 4B and 5B) indicate that the second part of FoxO4 NLS either directly interacts with the 14-3-3 protein or dramatically changes its conformation as a result of complex formation. We conclude that the binding of the 14-3-3 protein can affect the whole region of FoxO4 NLS.

It is now generally accepted that the dimeric nature of 14-3-3 proteins is crucial for their optimal function (*18*, *40*). Yaffe (*18*) suggested that the 14-3-3 dimer binds to its ligand

via a two-step mechanism. The first step involves the binding of one 14-3-3 monomer to a high-affinity binding site (the "gatekeeper"), thus enabling the binding of the second monomer to a low-affinity binding site, which would not bind individually. It is likely that both 14-3-3 binding motifs of FoxO factors are simultaneously used and required for the binding of FoxO factors to 14-3-3 proteins (*11*, *12*, *24*). However, it has also been speculated that the 14-3-3 protein might bind to one 14-3-3 binding motif of FoxO4 first and then the second motif can be used (*4*). Our fluorescence anisotropy decay measurements of AEDANS-labeled Cys^{213} of $FoxO4_{11-213}$ and $Trp^{173,174}$ of $FoxO4_{82-207}$ indicate that the DBD of FoxO4 remains relatively mobile while bound to the 14-3-3 protein. These observations could be interpreted in terms of the equilibrium between different complexes where phosphorylated FoxO4 is attached to the 14-3-3 protein using either only one PKB site or both.

Effect of DNA Binding. It has been suggested that the binding of 14-3-3 proteins may also affect the subcellular localization of FoxO factors by interfering with their ability to bind DNA (*11*, *37*). One of the potential regions where the 14-3-3 protein could interfere with the DNA binding is the C-terminal region of FoxO4 DBD. Our measurements showed that the binding of double-stranded DNA just slightly increases the polarity of the microenvironment around AEDANS-labeled Cys^{213} (Figures 4A and 5A) and has no significant effect on the flexibility of this FoxO4 region (Figure 8 and Table 1). These results suggest that the end of FoxO4 NLS in the vicinity of residue 213 does not participate in DNA binding. Therefore, the inhibitory effect of the 14-3-3 protein on DNA binding could be caused by interference in a different region of FoxO4 DBD.

Interaction between the 14-3-3 Protein and Unphosphorylated $FoxO4_{11-213}$. Although 14-3-3 proteins primarily bind phosphorylated ligands, they are also capable of interacting with unphosphorylated targets (*15*, *41*). The interaction of 14-3-3 proteins with unphosphorylated targets can be of high affinity, and it is likely that both unphosphorylated and phosphorylated ligands employ a similar ligand-binding site. Recently, performed biophysical characterization of interactions among the 14-3-3 protein, $FoxO4_{11-213}$, and its target DNA using sedimentation equilibrium revealed a weak interaction between the 14-3-3 protein and unphosphorylated $FoxO4_{11-213}$ with a K_D of 5−10 μM (*11*). This weak binding was not able to inhibit the interaction between FoxO4 and DNA. On the other hand, FoxO4 phosphorylation by PKB at Thr^{28} and Ser^{193} triggers high-affinity binding of $dpFoxO4_{11-213}$ to the 14-3-3 dimer with a K_D of 30 nM, leading to a complete inhibition of DNA binding (*11*). Results reported here are consistent with these data. Although fluorescence spectroscopy measurements show that some weak interaction exists between the 14-3-3 protein and AEDANS-labeled unphosphorylated $FoxO4_{11-213}$ (Figures 3A and 6), only high-affinity binding of the 14-3-3 protein to AEDANS-labeled phosphorylated $dpFoxO4_{11-213}$ (parts A and B of Figure 3) inhibits DNA binding (Figure 2A), significantly changes the polarity around Cys^{213}-AEDANS (Figures 4B and 5B), and reduces fast movements of AEDANS-labeled NLS (Table 1 and Figure 8). Moreover disruption of FoxO PKB phosphorylation sites is known to efficiently inhibit both the 14-3-3 protein binding and cytoplasmic relocalization *in vivo* (*9*, *10*, *12*, *24*). Therefore, it is likely that the weak interaction between unphosphorylated FoxO4 and the 14-3-3 protein observed *in vitro* does not play any role in the regulation of the FoxO4 function.

In conclusion, we have investigated structural changes of nuclear localization sequence of forkhead transcription factor FoxO4 induced by PKB phosphorylation, binding of the 14-3-3 protein and double-stranded DNA. Our data indicate that the 14-3-3 protein interacts with dpFoxO4 NLS and significantly affects its structure, while PKB phosphorylation itself and DNA binding have a negligible effect on the structure of this region. Our results also suggest that the DBD of dpFoxO4 remains relatively mobile while bound to the 14-3-3 protein.

ACKNOWLEDGMENT

We thank Dr. Gabrielle Grundy for critical reading of the manuscript. This work was funded by Grant 204/03/0714 of the Grant Agency of the Czech Republic, by Research Projects 1K03020, MSM 0021620835 and Centre of Neurosciences LC554 of the Ministry of Education, Youth, and Sports of the Czech Republic, and by Research Project AVOZ50110509.

REFERENCES

1. Weigel, D., and Jackle, H. (1990) The fork head domain: A novel DNA binding motif of eukaryotic transcription factors? *Cell 63*, 455−456.
2. Burgering, B. M., and Kops, G. J. (2002) Cell cycle and death control: Long live forkheads, *Trends. Biochem. Sci. 27*, 352−360.
3. Katoh, M., and Katoh, M. (2004) Human FOX gene family (review), *Int. J. Oncol. 25*, 1495−1500.
4. van der Heide, L. P., Hoekman, M. F., and Smidt, M. P. (2004) The ins and outs of FoxO shuttling: Mechanisms of FoxO translocation and transcriptional regulation, *Biochem. J. 380*, 297−309.
5. Weigelt, J., Climent, I., Dahlman-Wright, K., and Wikstrom, M. (2001) Solution structure of the DNA binding domain of the human forkhead transcription factor AFX (FOXO4), *Biochemistry 40*, 5861−5869.
6. Accili, D., and Arden, K. C. (2004) FoxOs at the crossroads of cellular metabolism, differentiation, and transformation, *Cell 117*, 421−426.
7. Jacobs, F. M., van der Heide, L. P., Wijchers, P. J., Burbach, J. P., Hoekman, M. F., and Smidt, M. P. (2003) FoxO6, a novel member of the FoxO class of transcription factors with distinct shuttling dynamics, *J. Biol. Chem. 278*, 35959−35967.
8. Arden, K. C., and Biggs, W. H., III (2002) Regulation of the FoxO family of transcription factors by phosphatidylinositol-3 kinase-activated signaling, *Arch. Biochem. Biophys. 403*, 292−298.
9. Brunet, A., Bonni, A., Zigmond, M. J., Lin, M. Z., Juo, P., Hu, L. S., Anderson, M. J., Arden, K. C., Blenis, J., and Greenberg, M. E. (1999) Akt promotes cell survival by phosphorylating and inhibiting a Forkhead transcription factor, *Cell 96*, 857−868.
10. Rena, G., Prescott, A. R., Guo, S., Cohen, P., and Unterman, T. G. (2001) Roles of the forkhead in rhabdomyosarcoma (FKHR) phosphorylation sites in regulating 14-3-3 binding, transactivation, and nuclear targetting, *Biochem. J. 354*, 605−612.
11. Obsil, T., Ghirlando, R., Anderson, D. E., Hickman, A. B., and Dyda, F. (2003) Two 14-3-3 binding motifs are required for stable association of Forkhead transcription factor FOXO4 with 14-3-3 proteins and inhibition of DNA binding, *Biochemistry 42*, 15264−15272.
12. Zhao, X., Gan, L., Pan, H., Kan, D., Majeski, M., Adam, S. A., and Unterman, T. G. (2004) Multiple elements regulate nuclear/cytoplasmic shuttling of FOXO1: Characterization of phosphorylation- and 14-3-3-dependent and -independent mechan, *Biochem. J. 378*, 839−849.
13. Muslin, A. J., Tanner, J. W., Allen, P. M., and Shaw, A. S. (1996) Interaction of 14-3-3 with signaling proteins is mediated by the recognition of phosphoserine, *Cell 84*, 889−897.

14. Muslin, A. J, and Xing, H. (2000) 14-3-3 proteins: Regulation of subcellular localization by molecular interference, *Cell. Signalling 12*, 703−709.
15. Fu, H., Subramanian, R. R., and Masters, S. C. (2000) 14-3-3 proteins: Structure, function, and regulation, *Annu. Rev. Pharmacol. Toxicol. 40*, 617−647.
16. Yaffe, M. B., and Elia, A. E. (2001) Phosphoserine/threonine-binding domains, *Curr. Opin. Cell Biol. 13*, 131−138.
17. Obsil, T., Ghirlando, R., Klein, D. C., Ganguly, S., and Dyda, F. (2001) Crystal structure of the 14-3-3ζ:serotonin *N*-acetyltransferase complex. A role for scaffolding in enzyme regulation, *Cell 105*, 257−267.
18. Yaffe, M. B. (2002) How do 14-3-3 proteins work? Gatekeeper phosphorylation and the molecular anvil hypothesis, *FEBS Lett. 513*, 53−57.
19. Lopez-Girona, A., Furnari, B., Mondesert, O., and Russell, P. (1999) Nuclear localization of Cdc25 is regulated by DNA damage and a 14-3-3 protein, *Nature 397*, 172−175.
20. Seimiya, H., Sawada, H., Muramatsu, Y., Shimizu, M., Ohko, K., Yamane, K., and Tsuruo, T. (2000) Involvement of 14-3-3 proteins in nuclear localization of telomerase, *EMBO J. 19*, 2652−2661.
21. Grozinger, C. M., and Schreiber, S. L. (2000) Regulation of histone deacetylase 4 and 5 and transcriptional activity by 14-3-3-dependent cellular localization, *Proc. Natl. Acad. Sci. U.S.A. 97*, 7835−7840.
22. Brownawell, A. M., Kops, G. J., Macara, I. G., and Burgering, B. M. (2001) Inhibition of nuclear import by protein kinase B (Akt) regulates the subcellular distribution and activity of the forkhead transcription factor AFX, *Mol. Cell. Biol. 21*, 3534−3546.
23. Zhang, X., Gan, L., Pan, H., Guo, S., He, X., Olson, S. T., Mesecar, A., Adam, S., and Unterman, T. G. (2002) Phosphorylation of serine 256 suppresses transactivation by FKHR (FOXO1) by multiple mechanisms. Direct and indirect effects on nuclear/cytoplasmic shuttling and DNA binding, *J. Biol. Chem. 277*, 45276−45284.
24. Brunet, A., Kanai, F., Stehn, J., Xu, J., Sarbassova, D., Frangioni, J. V., Dalal, S. N., DeCaprio, J. A., Greenberg, M. E., and Yaffe, M. B. (2002) 14-3-3 transits to the nucleus and participates in dynamic nucleocytoplasmic transport, *J. Cell. Biol. 156*, 817−828.
25. Kovarova, H., Halada, P., Man, P., Golovliov, I., Krocova, Z., Spacek, J., Purkertova, S., and Necasova, R. (2002) Proteome study of *Francisella tularensis* live vaccine strain-containing phagosome in Bcg/Nramp1 congenic macrophages: Resistant allele contributes to permissive environment and susceptibility to infection, *Proteomics 2*, 85−93.
26. Silhan, J., Obsilova, V., Vecer, J., Herman, P., Sulc, M., Teisinger, J., and Obsil, T. (2004) 14-3-3 protein C-terminal stretch occupies ligand binding groove and is displaced by phosphopeptide binding, *J. Biol. Chem. 279*, 49113−49119.
27. Palfner, K., Kneba, M., Hiddemann, W., and Bertram, J. (1995) Short technical reports. Quantification of ribozyme-mediated RNA cleavage using silver-stained polyacrylamide gels, *BioTechniques 19*, 926−929.
28. Obsilova, V., Herman, P., Vecer, J., Sulc, M., Teisinger, J., and Obsil, T. (2004) 14-3-3ζ C-terminal stretch changes its conformation upon ligand binding and phosphorylation at Thr232, *J. Biol. Chem. 279*, 4531−4540.
29. Bryan, R. K. (1990) Maximum-entropy analysis of oversampled data problems, *Eur. Biophys. J. 18*, 165−174.
30. Brochon, J. C. (1994) Maximum entropy method of data analysis in time-resolved spectroscopy, *Methods Enzymol. 240*, 262−311.
31. Rischel, C., Thyberg, P., Rigler, F., and Poulsen, F. M. (1996) Time-resolved fluorescence studies of the molten globule state of apomyoglobin, *J. Mol. Biol. 257*, 877−885.
32. Belford, G. G., Belford, R. L., and Weber, G. (1972) Dynamics of fluorescence polarization in macromolecules, *Proc. Natl. Acad. Sci. U.S.A. 69*, 1392−1393.
33. Lakowicz, J. R. (1999). *Principles of Fluorescence Spectroscopy*, Kluwer Academic/Plenum Publisher, New York.
34. Yguerabide, J., Epstein, H. F., and Stryer, L. (1970) Segmental flexibility in an antibody molecule, *J. Mol. Biol. 51*, 573−590.
35. Kawski, A. (1993) Fluorescence anisotropy—Theory and applications of rotational depolarization, *Crit. Rev. Anal. Chem. 23*, 459−529.
36. Eftink, M. R. (2000) in *Topics in Fluorescence Spectroscopy* (Lakowicz, J. R., Ed.) Vol. 6, pp 1−15, Kluwer Academic/Plenum Publisher, New York.
37. Cahill, C. M., Tzivion, G., Nasrin, N., Ogg, S., Dore, J., Ruvkun, G., and Alexander-Bridges, M. (2001) Phosphatidylinositol 3-kinase signaling inhibits DAF-16 DNA binding and function via 14-3-3-dependent and 14-3-3-independent pathways, *J. Biol. Chem. 276*, 13402−13410.
38. Yaffe, M. B., Rittinger, K., Volinia, S., Caron, P. R., Aitken, A., Leffers, H., Gamblin, S. J., Smerdon, S. J., and Cantley, L. C. (1997) The structural basis for 14-3-3:phosphopeptide binding specificity, *Cell 91*, 961−971.
39. Rittinger, K., Budman, J., Xu, J., Volinia, S., Cantley, L. C., Smerdon, S. J., Gamblin, S. J., and Yaffe, M. B. (1999) Structural analysis of 14-3-3 phosphopeptide complexes identifies a dual role for the nuclear export signal of 14-3-3 in ligand binding, *Mol. Cell 4*, 153−166.
40. Tzivion, G., Luo, Z., and Avruch, J. (1998) A dimeric 14-3-3 protein is an essential cofactor for Raf kinase activity, *Nature 394*, 88−92.
41. Masters, S. C., Pederson, K. J., Zhang, L., Barbieri, J. T., and Fu, H. (1999) Interaction of 14-3-3 with a nonphosphorylated protein ligand, exoenzyme S of *Pseudomonas aeruginosa*, *Biochemistry 38*, 5216−5221.

BI050618R